Easy-plane XY spin fluctuations in the cycloidal magnet UPtGe studied via field-orientation-dependent ^{195}Pt NMR

Y. Tokunaga,[1,*] A. Nakamura,[2] D. Aoki,[2] Y. Shimizu,[2] Y. Homma,[2] F. Honda,[2] H. Sakai,[1] T. Hattori,[1] and S. Kambe[1]
[1]*ASRC, Japan Atomic Energy Agency, Tokai, Ibaraki 319-1195, Japan*
[2]*IMR, Tohoku University, Ibaraki 311-1313, Japan*

(Received 21 April 2018; revised manuscript received 27 May 2018; published 23 July 2018)

^{195}Pt NMR measurements have been performed on a single crystal of the uranium-based compound UPtGe, which is the only 5f system known to possess an incommensurate helical (cycloidal) structure below $T_N = 50$ K. Knight shift measurement confirmed the isotropic character of the static spin susceptibilities in hexagonal-like ac crystal planes of the EuAuGe-type crystal structure. The hyperfine coupling constants were also found to be isotropic in the planes, estimated to be 59 kOe/μ_B. Nuclear relaxation rate ($1/T_1$) measurement revealed the development of the antiferromagnetic spin fluctuations with XY character confined to the hexagonal-like plane below 200 K. The results present a clear contrast to the Ising anisotropy of the fluctuations in ferromagnetic superconductors UCoGe and URhGe.

DOI: 10.1103/PhysRevB.98.014425

I. INTRODUCTION

The series of UTGe germanides have attracted considerable attention after the discovery of superconductivity in the ferromagnetic (FM) state of UCoGe [1] and URhGe [2]. Except for T=Ru and Fe, the UTGe germanides exhibit static, long-range ordering of the U 5f spin moments. While UCoGe and URhGe are both simple ferromagnets with transition temperatures of 3 K [1,3] and 9.5 K [2], the heavier transition elements (T = Ni, Pd, and Pt) introduce rather complex magnetic structure with relatively higher transition temperatures of around 50 K [4–7]. UNiGe, for example, possesses two different antiferromagnetic (AFM) phases. The magnetic structure between 42 K and $T_N = 50$ K is incommensurate, while it changes to commensurate below 42 K [4,8,9]. On the other hand, UPdGe has a longitudinal, sinusoidal AFM structure between 28 and 50 K, while it transforms to a ferromagnet at 28 K [5,7,10,11].

The most peculiar magnetic structure in the UTGe series appears in UPtGe [4,10,12–15]. Below $T_N = 50$ K, the compound exhibits an incommensurate helical (=cycloidal) order with the propagation vector $q = (0.55–0.57,0,0)$, where the U moments of $\sim 1.4\mu_B$ lie in the deformed hexagonal plane and are aligned ferromagnetically between the planes (Fig. 1) [14]. In general, the helical magnetic structure has a periodicity incommensurate with the periodicity of the crystal lattice [16]. The helical structure is thus naturally conflicted via the strong spin-orbit coupling, which connects the space and spin degrees of freedom, and hence tends to generate different, inequivalent orientations of the moments with respect to the lattice. This implies that helical order is not a very likely ground state for actinide compounds, where the 5f electrons possess strong spin-orbit coupling [17,18]. Up to now, UPtGe is the only actinide system known to exhibit helical structure [16].

In this paper, we report a microscopic investigation of magnetic anisotropy and fluctuations in UPtGe. Orientation-dependent ^{195}Pt NMR results obtained with a high-quality single crystal have confirmed a two-dimensional, easy-plane character for both the static and dynamical susceptibilities in the paramagnetic state. The NMR measurements also exhibit a small magnetic anisotropy in the plane, satisfying a necessary condition for the formation of a unique cycloidal order in this compound. The behaviors present a clear contrast to the strong Ising anisotropy of the magnetization in ferromagnetic superconductors UCoGe [19,20] and URhGe [21–23]. UPtGe appears to be an interesting material to understand why the spin reorientation and FM instabilities occur in URhGe.

II. EXPERIMENTAL METHOD

Single crystals of UPtGe were grown using the Czochralski pulling method. The magnetic susceptibility data of our crystals well reproduce the previous results, showing a clear anomaly for the magnetic phase transition at $T_N = 50$ K [7,15]. The ^{195}Pt NMR measurements were carried out on a single crystal ($3 \times 1.5 \times 1.5$ mm size) using a superconducting magnet and a phase coherent, pulsed spectrometer. The ^{195}Pt nuclei have a natural abundance of 33.8% and the nuclear gyromagnetic ratio $\gamma_N/2\pi = 9.094$ MHz/T ($S = 1/2$). The NMR spectrum was measured at several different temperatures by recording integrated spin-echo intensities while sweeping the external field $H \sim 9$ T. The temperature dependence of the NMR (Knight) shift K_α was derived from the peak position of the NMR spectrum with field applied along the three respective orthorhombic crystal axes ($\alpha = a, b$, and c), where Cu-NMR signals from metallic copper were used as makers for field calibrations. The spin-lattice relaxation rate $1/T_{1\alpha}$ was also measured at several different temperatures with H along the three axes. The measured nuclear magnetization recovery was found to fit a simple exponential for these $I = 1/2$ nuclei, allowing us to determine a unique T_1 value at each temperature.

*tokunaga.yo@jaea.go.jp

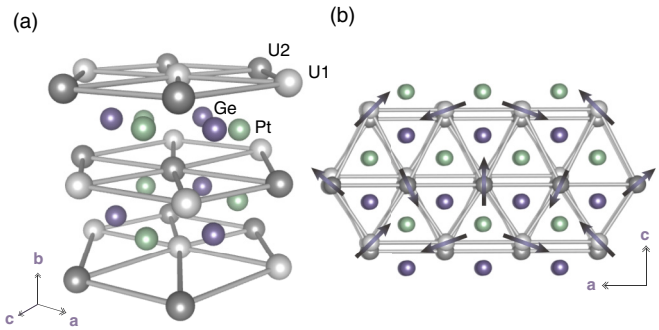

FIG. 1. Schematic view of the EuAuGe crystal structure of UPtGe. (a) The structure involves orthorhombically deformed hexagonal-form ac planes delineated by the two different uranium sites, U1 and U2. (b) The projection onto the ac plane showing the cycloidal structure of the U moments in the ordered state (only the cycloid in one upper ac plane is shown) [10,15,16]. The b axis is vertical to the plane.

III. EXPERIMENTAL RESULTS

A. Temperature dependence of the NMR shift

The crystal structure of UPtGe was initially suggested to be the TiNiSi type, the same as the other UTGe compounds [12]. However, subsequent neutron experiments showed that a better description of the data was obtained using the EuAuGe-type structure (Fig. 1) with space group $Imm2$ (No. 44, C_{2v}^{20}) [14,15,24]. The $Imm2$ space group is noncentrosymmetric, whereas the $Pnma$ space group of the TiNiSi-type structure is centrosymmetric. Both structures have U atoms at essentially the same positions; only the configurations of Pt and Ge atoms vary between these structures. Note that the a and b axes are interchanged in going from the $Pnma$ to $Imm2$ space groups. The a, b, and c axes in the EuAuGe-type structure correspond to the b, a, and c axes in the TiNiSi-type structure, respectively.

Figure 2 exhibits the temperature dependence of ^{195}Pt NMR spectra obtained with H along the a axis. A narrow peak

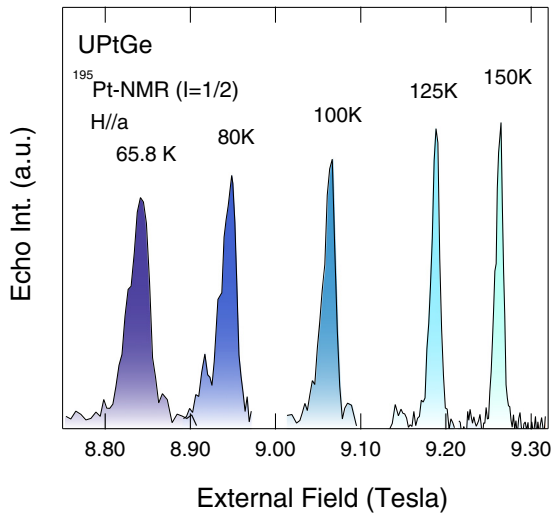

FIG. 2. Temperature dependence of the ^{195}Pt NMR spectrum in the paramagnetic state. The spectra were measured with the field applied along the a axis. The FWHM is ~0.01 T at 150 K.

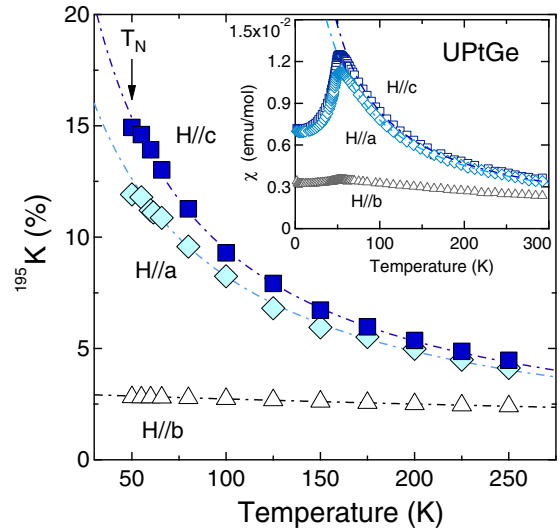

FIG. 3. Temperature dependence of the NMR (Knight) shift for fields applied along the three crystalline axes. The dashed lines are the results of Curie-Weiss fits $K_\alpha \propto C/(T-\theta_\alpha)$. The inset shows the temperature dependence of the bulk magnetic susceptibility (χ_α). The dashed lines are the results of a modified Curie-Weiss law, $\chi_\alpha = \chi_v^\alpha + C/(T-\theta'_\alpha)$, which provides $\theta'_{a,c} = -28$ K and -15 K with $\chi_v^{a,c} = 3.6\times10^{-4}$ and 3.8×10^{-4} emu/mol for $H\|a$ and c, respectively.

at high temperatures indicates the high quality of our single crystals. At decreasing temperatures, the spectrum broadens and shifts to lower fields (to a larger Knight shift). This gradual broadening is attributed to a distribution of the Knight shift, since ^{195}Pt nuclei of $I = 1/2$ have no quadrupolar broadening.

In Fig. 3, we show the temperature dependence of the Knight shift for fields applied along all three crystal axis directions. With decreasing temperature, both K_a and K_c exhibit a rapid increase while following a Curie-Weiss (CW) law, as shown by the broken lines in the figure. The CW fits provide Curie temperatures $\theta_{a,c} = -44$ and -30 K for $H\|a$ and c, respectively. By contrast, measured values of K_b are much smaller and nearly temperature independent [15]. The large anisotropy of K_α for H in and out of plane has essentially the same origin as the anisotropy of bulk magnetic susceptibility (χ_α), as shown in the inset to Fig. 3 [7,15]. The Knight shifts also confirm very small in-plane anisotropy within the ac plane.

For the f-electron systems the Knight shift is generally composed of a spin part $K^{\rm s}$ and a Van Vleck part $K^{\rm v}$. These components are connected with a T-dependent spin susceptibility $\chi^{\rm s}$ and a T-independent Van Vleck susceptibility $\chi^{\rm v}$ as

$$K(T) = K^{\rm s}(T) + K^{\rm v} = \frac{1}{N_{\rm A}\mu_{\rm B}}\left(A_{\rm hf}^{\rm s}\chi^{\rm s}(T) + A_{\rm hf}^{\rm v}\chi^{\rm v}\right), \quad (1)$$

where $A_{\rm hf}^{\rm s(v)}$ is the spin (Van Vleck) part of the hyperfine (HF) coupling constant, $N_{\rm A}$ is Avogadro's number, and $\mu_{\rm B}$ the Bohr magneton. In Fig. 4, we plot K_α against χ_α with temperature as an implicit variable. The data points nearly lie on a single line, confirming the isotropic character of the dominating HF

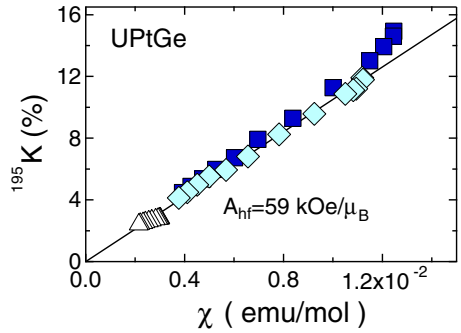

FIG. 4. The Knight shifts are plotted against the bulk susceptibility χ with temperature as an implicit parameter. The slopes of the dashed lines correspond to an isotropic hyperfine coupling constant of 59 kOe/μ_B.

mechanism. The slope of the single line yields the isotropic transferred HF coupling constants $A^s_{hf} \simeq 59$ kOe/μ_B. On the other hand, the intersection of the line at $\chi = 0$ is nearly zero. In UPtGe, the susceptibility measurements indicate that $\chi_v \simeq 0$, and hence, K^v should be $\simeq 0$ as observed. The isotropic HF coupling implies the predominance of U 5f spin moment transfer to Pt 6s orbitals which interact directly with Pt nuclei. The anisotropic couplings such as the dipolar term seem to give only minor contributions. A similar situation has been found in other UTGe compounds, e.g., in UCoGe, where the isotropic HF coupling at Co nuclei is given by a spin transfer from U 5f to Co 4s orbitals [19].

B. The spin-lattice relaxation time T_1

Figure 5 shows the temperature dependence of $(1/T_1)_\alpha$ measured in our single-crystal sample with the field applied in turn along the three respective orthorhombic crystal axes, $\alpha = a$, b, and c. It is noteworthy that $1/T_1$ exhibits a different temperature dependence for $(1/T_1)_b$, in contrast with $(1/T_1)_{a,c}$. At temperatures above 200 K, $1/T_1$ is nearly isotropic. However,

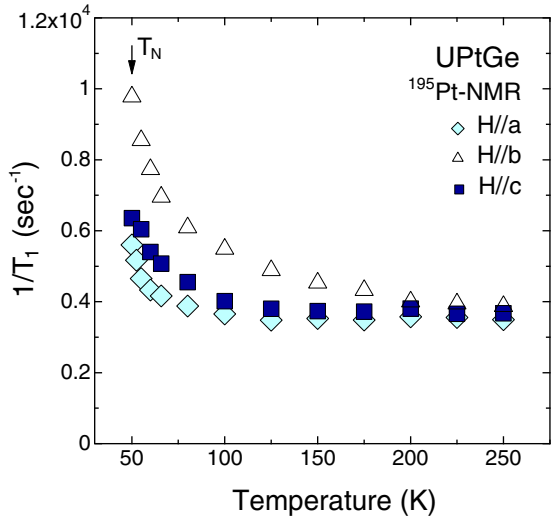

FIG. 5. The temperature dependence of $1/T_1$ for ^{195}Pt, measured with fields applied along the three mutually orthogonal crystalline axes as indicated.

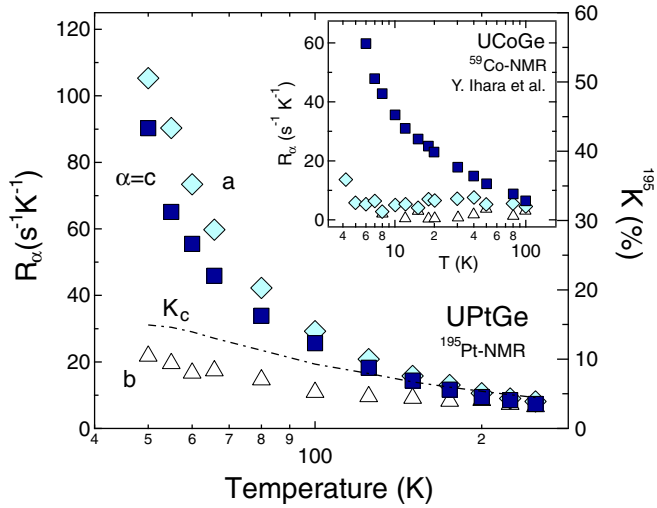

FIG. 6. Orientation-resolved dynamic susceptibility R_α (see text) along the three crystalline axis directions in UPtGe. The inset shows R_α reported in UCoGe [19]. Note that the a and b axes in UCoGe with the TiNiSi structure are interchanged with respect to those in UPtGe.

with decreasing temperature, mainly $(1/T_1)_b$ increases gradually below 200 K, while $(1/T_1)_{a,c}$ remains nearly constant down to 100 K. While $(1/T_1)_{a,c}$ show a modest increase below 100 K, their values are only about half of $(1/T_1)_b$ for $T \sim T_N$. Since $1/T_1$ is determined by spin fluctuations perpendicular to the quantization axis of the nuclear spins, i.e., the fixed field axis, the rapid increase of $(1/T_1)_b$ indicates the development of spin and hyperfine field fluctuations in the ac plane.

The general expression for $1/T_1$ measured in a field along the α direction may be written [19,25]

$$\left(\frac{1}{T_1T}\right)_\alpha = \frac{\gamma_n^2 k_B}{2}\sum_{\boldsymbol{q}}\left[\left|A^{s,\beta}_{hf}\right|^2\frac{\chi''_\beta(\boldsymbol{q},\omega_n)}{\omega_n} + \left|A^{s,\gamma}_{hf}\right|^2\frac{\chi''_\gamma(\boldsymbol{q},\omega_n)}{\omega_n}\right], \quad (2)$$

where $\chi''_{\beta,\gamma}(\boldsymbol{q},\omega_n)$ is the imaginary part of the dynamic susceptibility along the β and γ directions perpendicular to α, ω_n is the NMR resonance frequency, and A^s_{hf} is the s-contact hyperfine coupling constant for the ^{195}Pt nucleus. In this way, we can evaluate the directional dynamic susceptibility components for each orthorhombic crystal axis,

$$R_\alpha = \sum_{\boldsymbol{q}}\left|A^{s,\alpha}_{hf}\right|^2\frac{\chi''_\alpha(\boldsymbol{q},\omega_n)}{\omega_n}, \quad (3)$$

using the relations $(1/T_1T)_a = R_b + R_c$, $(1/T_1T)_b = R_a + R_c$, and $(1/T_1T)_c = R_a + R_b$. The results are shown in Fig. 6.

The figure clearly demonstrates strong, easy-plane anisotropy for the dynamical spin susceptibilities, i.e., $R_a \simeq R_c \gg R_b$. The strong increase of both R_a, R_c with decreasing temperature indicates the development of the spin fluctuations with XY-type character in the ac plane. Furthermore, we can see that its temperature dependence does not scale with that of the Knight shift, which is proportional to $\chi(q = 0)$; $R_{a,c}(T)$ shows a much stronger increase than $K_{a,c}(T)$ below 200 K.

This suggests the dominance of the AFM components (i.e., $q \neq 0$) for the spin fluctuations in UPtGe.

The static and dynamical spin susceptibilities often possess contrasting anisotropies in f-electron systems [26–29]. In the present case, however, we found the same anisotropy for them. Furthermore, the easy-plane XY-type character of the fluctuations in UPtGe present a strong contrast to the Ising fluctuations in UCoGe and URhGe [19–23]. In the inset of Fig. 6, we show the temperature dependence of $R_{a,b,c}$ reported by Ihara *et al.* for UCoGe [19]. Only R_c exhibits a strong increase toward the FM transition at 3 K, while R_a and R_b are nearly constant in all the temperature range. Thus the spin fluctuations have a strong Ising character in UCoGe. The Ising fluctuations are suggested to be responsible for the FM superconductivity below ∼0.8 K [19,20].

IV. DISCUSSION AND SUMMARY

A characteristic feature of the UTGe germanides is strong magnetic anisotropy relative to their crystal structures. Both the TiNiSi- and EuAuGe-type structures can be considered as a kind of orthorhombically deformed hexagonal structure (Fig. 1). The a (b) axis of the TiNiSi (EuAuGe) lattice corresponds to the hexagonal c axis of the AlB_2 lattice. U atoms form zigzag chains along the a (b) direction (perpendicular to the planes). It has been found for all the UTGe series that the direction along the zigzag chain is always magnetically much harder than the other two axes [7,15,30]. This has also been confirmed by the present NMR results for both the static and dynamical spin susceptibilities in UPtGe.

On the other hand, the magnetocrystalline anisotropy within the hexagonal-like planes (i.e., the ac planes in UPtGe while the bc planes in the other UTGe compounds) depends strongly on the particular transition element T. The anisotropy becomes larger with the lighter transition elements, such as Co and Rh, providing a strong in-plane uniaxial anisotropy, i.e., $\chi_c \gg \chi_b > \chi_a$ [1,2]. On the other hand, it becomes much weaker with the presence of heavier transition elements. In particular, we show here in UPtGe that both the static and dynamical spin susceptibilities are nearly isotropic in the planes (see Figs. 3 and 6). It is evident that such a small in-plane anisotropy provides a necessary condition for the formation of incommensurate cycloidal order [16].

With decreasing temperature, magnetic correlations develop in the plane, driving the easy-plane XY spin fluctuations in UPtGe. This poses a clear contrast to the case of UCoGe and URhGe, where Ising-like fluctuations are suggested to generate superconductivity in the FM state [19–23]. It is also known that the in-plane Ising anisotropy in URhGe is slightly weaker than that in UCoGe, and then, a magnetic field (∼12 T) applied along the b axis forces the FM order to align to the field direction [31]. The fluctuations associated with this spin reorientation in the planes cause a reentrant superconductivity in URhGe [21–23]. It has been found that UPtGe also shows metamagnetic transitions for the fields applied along the hexagonal-like planes [32,33]. It will be important to understand why the Ising anisotropy depends strongly on the transition element, with its consequences to metamagnetic transitions in UTGe.

As for the origin of the unique cycloidal order, a theoretical study has been performed by Sandratskii and Lander within density functional theory [16]. They suggest that the EuAuGe-type structure of UPtGe leads to accidentally small in-plane magnetic anisotropy; thus, the formation and properties of the cycloidal structure are determined by frustrated exchange interactions, together with the relativistic Dzyaloshinskii-Moriya interaction [34]. The frustrated interactions were suggested to occur in the ac planes with a hexagonal-form lattice.

So far, we have not succeeded in observing NMR signals below T_N, and thus, we cannot discuss whether frustrated interactions indeed exist or not in UPtGe. In the ordered state, it has been proposed that the absence of anisotropy in the ac plane would give rise to a Goldstone mode in the spin-wave excitations with the cycloidal structure [16]. We suggest that further NMR studies, and in particular measurements conducted under uniaxial pressure to control the degree of deformation of the hexagonal lattice in the ac planes [35], would be desirable to clarify these points.

ACKNOWLEDGMENTS

We would like to thank R. E. Walstedt for valuable discussions and a critical reading of our manuscript. A part of this work was supported by JSPS KAKENHI [Grants No. JP15KK0174, No. JP15H05745, No. JP15H05884 (J-Physics), and No. JP16H04006], ICC-IMR, and the REIMEI Research Program of JAEA.

[1] N. T. Huy, A. Gasparini, D. E. de Nijs, Y. Huang, J. C. P. Klaasse, T. Gortenmulder, A. de Visser, A. Hamann, T. Gorlach, and H. von Lohneysen, Phys. Rev. Lett. **99**, 067006 (2007).

[2] D. Aoki, A. Huxley, E. Ressouche, D. Braithwaite, J. Flouquet, J.-P. Brison, E. Lhotel, and C. Paulsen, Nature (London) **413**, 613 (2001).

[3] A. Gasparini, Y. K. Huang, N. T. Huy, J. C. P. Klaasse, T. Naka, E. Slooten, and A. de Visser, J. Low Temp. Phys. **161**, 134 (2010).

[4] V. Sechovsky and L. Havela, in *Handbook of Magnetic Materials*, edited by K. H. J. Buschow (North-Holland, Amsterdam, 1998), Vol. 11, p. 93.

[5] R. Troć and V. H. Tran, J. Magn. Magn. Mater. **73**, 389 (1988).

[6] L. Havela, A. Kolomiets, V. Sechovsky, M. Divis, M. Richter, and A. V. Andreev, J. Magn. Magn. Mater. **177-181**, 47 (1988).

[7] S. Kawamata, K. Ishimoto, H. Iwasaki, N. Kobayashi, Y. Yamaguchi, T. Komatsubara, G. Kido, T. Mitsugashira, and Y. Muto, J. Magn. Magn. Mater. **90-91**, 513 (1990).

[8] H. Nakotte, A. Purwanto, R. A. Robinson, Z. Tun, K. Prokes, A. C. Larson, L. Havela, V. Sechovsky, H. Maletta, E. Brück, and F. R. de Boer, Phys. Rev. B **54**, 7201 (1996).

[9] K. Prokeš, P. F. de Châtel, E. Brück, F. R. de Boer, K. Ayuel, H. Nakotte, and V. Sechovský, Phys. Rev. B **65**, 144429 (2002).

[10] S. Kawamata, K. Ishimoto, Y. Yamaguchi, and T. Komatsubara, J. Magn. Magn. Mater. **104-107**, 51 (1992).

[11] S. El-Khatib, S. Chang, H. Nakotte, D. Brown, E. Brück, A. J. Schultz, A. Christianson, and A. Lacerda, J. Appl. Phys. **93**, 8352 (2003).
[12] A. Szytula, M. Kolenda, R. Troc, V. H. Tran, M. Bonnet, and J. Rossat-Mignod, Solid State Commun. **81**, 481 (1992).
[13] R. A. Robinson, A. C. Lawson, J. W. Lynn, and K. H. J. Buschow, Phys. Rev. B **47**, 6138 (1993).
[14] D. Mannix, S. Coad, G. H. Lander, J. Rebizant, P. J. Brown, J. A. Paixao, S. Langridge, S. Kawamata, and Y. Yamaguchi, Phys. Rev. B **62**, 3801 (2000).
[15] R. Troć, J. Stepień-Damm, C. Sulkowski, and A. M. Strydom, Phys. Rev. B **69**, 094422 (2004).
[16] L. M. Sandratskii and G. H. Lander, Phys. Rev. B **63**, 134436 (2001).
[17] L. M. Sandratskii and J. Kübler, Mod. Phys. Lett. B **10**, 189 (1996).
[18] L. M. Sandratskii, Adv. Phys. **47**, 91 (1998).
[19] Y. Ihara, T. Hattori, K. Ishida, Y. Nakai, E. Osaki, K. Deguchi, N. K. Sato, and I. Satoh, Phys. Rev. Lett. **105**, 206403 (2010).
[20] T. Hattori, Y. Ihara, Y. Nakai, K. Ishida, Y. Tada, S. Fujimoto, N. Kawakami, E. Osaki, K. Deguchi, N. K. Sato, and I. Satoh, Phys. Rev. Lett. **108**, 066403 (2012).
[21] Y. Tokunaga, D. Aoki, H. Mayaffre, S. Krämer, M.-H. Julien, C. Berthier, M. Horvatić, H. Sakai, S. Kambe, and S. Araki, Phys. Rev. Lett. **114**, 216401 (2015).
[22] H. Kotegawa, K. Fukumoto, T. Toyama, H. Tou, H. Harima, A. Harada, Y. Kitaoka, Y. Haga, E. Yamamoto, Y. Ōnuki, K. M. Itoh, and E. E. Haller, J. Phys. Soc. Jpn. **84**, 054710 (2015).
[23] Y. Tokunaga, D. Aoki, H. Mayaffre, S. Krämer, M.-H. Julien, C. Berthier, M. Horvatić, H. Sakai, T. Hattori, S. Kambe, and S. Araki, Phys. Rev. B **93**, 201112(R) (2016).
[24] R.-D. Hoffmann, R. Pöttgen, G. H. Lander, and J. Rebizant, Solid State Sci. **3**, 697 (2001).
[25] T. Moriya, J. Phys. Soc. Jpn. **18**, 516 (1963).
[26] S. Kambe, H. Sakai, Y. Tokunaga, T. Fujimoto, R. E. Walstedt, S. Ikeda, D. Aoki, Y. Homma, Y. Haga, Y. Shiokawa, and Y. Ōnuki, Phys. Rev. B **75**, 140509(R) (2007).
[27] H. Sakai, S. Kambe, Y. Tokunaga, Y. Haga, S.-H. Baek, F. Ronning, E. D. Bauer, and J. D. Thompson, MRS Proceedings **1264**, Z12 (2010).
[28] S.-H. Baek, H. Sakai, E. D. Bauer, J. N. Mitchell, J. A. Kennison, F. Ronning, and J. D. Thompson, Phys. Rev. Lett. **105**, 217002 (2010).
[29] H. Sakai, H. Chudo, Y. Tokunaga, S. Kambe, Y. Haga, F. Ronning, E. D. Bauer, J. D. Thompson, Y. Homma, D. Aoki, Y. Nakano, F. Honda, R. Settai, and Y. Ōnuki, J. Phys. Soc. Jpn. Suppl. B **81**, SB003 (2012).
[30] M. Marutzky, U. Barkow, S. Weber, J. Schoenes and R. Troć, Phys. Rev. B **74**, 205115 (2006).
[31] F. Lévy, I. Sheikin, B. Grenier, and A. Huxley, Science **309**, 1343 (2005).
[32] S. Kawamata, G. Kido, K. Ishimoto, Y. Yamaguchi, H. Iwasaki, N. Kobayashi, and T. Komatsubara, Physica B **177**, 169 (1992).
[33] A. Miyake *et al.* (unpublished).
[34] I. Dzyaloshinskii, J. Phys. Chem. Solids **4**, 241 (1958); T. Moriya, Phys. Rev. **120**, 91 (1960).
[35] D. Braithwaite, D. Aoki, J.-P. Brison, J. Flouquet, G. Knebel, A. Nakamura, and A. Pourret, Phys. Rev. Lett. **120**, 037001 (2018).